ELSEVIER

Chemical Geology 186 (2002) 139–149

CHEMICAL GEOLOGY
INCLUDING
ISOTOPE GEOSCIENCE

www.elsevier.com/locate/chemgeo

Provenance of lithogenic surface sediments and pathways of riverine suspended matter in the Eastern Mediterranean Sea: evidence from $^{143}Nd/^{144}Nd$ and $^{87}Sr/^{86}Sr$ ratios

Syee Weldeab [a,b,*], Kay-Christian Emeis [b], Christoph Hemleben [a], Wolfgang Siebel [c]

[a] *Institute for Geosciences, University of Tübingen, Sigwartstr. 10, D-72076 Tübingen, Germany*
[b] *Institute for Baltic Sea Research Warnemünde, Seestr. 15, D-18119 Rostock-Warnemünde, Germany*
[c] *Institute for Mineralogy, Petrology, and Geochemistry, University of Tübingen, Wilhelmstr. 56, D-72074 Tübingen, Germany*

Received 11 May 2001; accepted 3 December 2001

Abstract

In order to characterize the provenance of lithogenic surface sediments from the Eastern Mediterranean Sea (EMS), residual (leached) fraction of 34 surface samples have been analysed for their $^{143}Nd/^{144}Nd$ and $^{87}Sr/^{86}Sr$ isotope ratios. The sample locations bracket all important entrances of riverine suspended matter into the EMS as well as all sub-basins of the EMS. The combined analyses of these two isotope ratios provide a precise characterization of the lithogenic fraction of surface sediments and record their dilution towards the central sub-basins. We reconstruct provenance and possible pathways of riverine dispersal and current redistribution, assuming more or less homogenous isotopic signatures and flux rates of the eolian fraction over the EMS. Lithogenic sediments entering the Ionian Sea from the Calabrian Arc and the Adriatic Sea are characterized by high $^{87}Sr/^{86}Sr$ isotope ratios and low $\varepsilon_{Nd(0)}$ values (average $^{87}Sr/^{86}Sr = 0.718005$ and $\varepsilon_{Nd(0)} = -11.06$, $n = 5$). Aegean Sea terrigenous sediments show an average ratio of $^{87}Sr/^{86}Sr = 0.713089$ ($n = 5$) and values of $\varepsilon_{Nd(0)} = -7.89$ ($n = 5$). The Aegean isotopic signature is traceable up to the southwest, south, and southeast of Crete. The sediment loads entering the EMS via the Aegean Sea are low and spread out mainly through the Strait of Casos (east of Crete). Surface sediments from the eastern Levantine Basin are marked by the highest $\varepsilon_{Nd(0)}$ values (-3.3, $n = 6$) and lowest $^{87}Sr/^{86}Sr$ isotope ratios (average 0.709541, $n = 6$), reflecting the predominant input of the Nile sediment. The influence of the Nile sediment is traceable up to the NE-trending, eastern flank of the Mediterranean Ridge. The characterization of the modern riverine dispersal and eolian flux, based on isotope data, may serve as a tool to reconstruct climate-coupled variations of lithogenic sediment input into the EMS.

Keywords: Eastern Mediterranean Sea; Nd-isotope ratios; Sr-isotope ratios; Lithogenic surface sediments; Provenance; Pathways

1. Introduction

The Eastern Mediterranean Sea (EMS) is bordered to the south and east by the North African desert belts and the Middle East desert, respectively. Those

* Corresponding author. Institut und Museum fur Geologie und Palaeontologie, Universitaet Tübingen, Sigwartstrasse 10, D-72076 Tübingen, Germany. Fax: +49-7071-295727.
E-mail address: syee.weldeab@uni-tuebingen.de (S. Weldeab).

0009-2541/02/$ - see front matter
PII: S0009-2541(01)00415-6

deserts are the most dominant sediment suppliers to the Mediterranean Sea due to wind erosion of its surface deposits and prevailing meteorological conditions. Dust storms relevant for the EMS emanate from areas consisting of Precambrian rocks and Cretaceous sandstone as well as their erosion products (D'Almeida, 1986). Mineralogical and geochemical analyses of the Saharan dust, collected over the EMS, indicate predominance of quartz, kaolinite, palygorskite, illite, and Fe- and Al-oxides (Chester et al., 1977; Tomadin et al., 1984; Guerzoni et al., 1997; Rutten et al., 2000). The isotope composition of the Saharan dusts is characterized by high $^{87}Sr/^{86}Sr$ ratios and low $\varepsilon_{Nd(0)}$ values (Grousset et al., 1998; Krom et al., 1999a). However, within the Mediterranean Sea, a slight E–W Sr isotopic gradient has been reported (Krom et al., 1999a). The second important source for detrital sediments entering the EMS is riverine suspended matter. The amount and geochemical composition of the riverine matter depends on the extent of the catchment areas and exposed rocks, respectively. The Nile river is by far the largest river system discharging into the EMS, with annual runoff of 91 km^3 and a sediment load of $\sim 60 \times 10^6$ tons/year (Krom, personal communication; Foucault and Stanley, 1989). Clay mineralogy and isotopic composition of the detritus brought by the Nile river are characterized by weathering products of basalt and the isotope signature of young basaltic rocks in the Ethiopian Highland (Venkatarathnam and Ryan, 1972; Goldstein et al., 1984; Krom et al., 1999a). However, since the construction of the High Dam at Aswan in 1964, slight mineralogical and textural changes in the delta and coastal areas and a reduction of the sediment input to the Levantine Basin have been observed (Stanley and Wingerath, 1996; Stanley et al., 1997, 1998).

Small rivers discharge into the Aegean Sea along the northern borderlands of the EMS. Aksu et al. (1995) suggests an annual sediment supply of 229 million tons from these sources to the Aegean Sea. However, this value might be an over estimation. The geology of the drainage areas consists of Tertiary basalts ultramafic rocks, Cretaceous–Paleocene limestones and schists in the north, and basaltic rocks of Tertiary–Quaternary ages as well as limestone in the east (western Turkey). Suspended matters of the Black Sea outflow may contribute to the sediment budget of the Aegean Sea. Quantitative estimations, however, are not available. The riverine sediment loads from the Aegean Sea entering into the EMS mainly mirror erosion product of basalts and ultramafic rocks (Venkatarathnam and Ryan, 1972; McCoy, 1974). In the eastern borderlands, there are no important rivers that could yield significant amount of sediments, and the contribution of ephemeral rivers is limited to the immediate vicinity of the coastal areas (Chester et al., 1977). The river Po, which drains the southern watershed of the Swiss, Austrian, and Italian Alps, discharges into the Adriatic Sea and a significant amount of Po-derived detritus may enter into the Ionian Sea via the Adriatic Sea (Fig. 1).

The EMS harbours one of the most prominent cyclic recurring sedimentary records of abrupt climate changes in the lower to middle latitude, the sapropels (e.g. Emeis et al., 2000). However, the exact conditions leading to the sapropel formation are still under debate (see Cramp and O'Sullivan, 1999 for review). Sr- and Nd-isotope analyses of the lithogenic component of the sapropels and intervening sediments are promising proxies for semiquantitative/quantitative reconstruction of variation of the lithogenic components (Krom et al., 1999b; Freydier et al., 2001; Weldeab et al., in press). Hence, they allow one to decipher the prevailing transport mechanisms and climatic conditions in catchment areas. Characterization of the EMS surface sediments and assessment of the riverine inputs from different sources, as well as eolian flux are a prerequisite for an isotope-based reconstruction of climate-coupled variations of older sediment sequences. Presently, the Nile river, Saharan dust, and rivers from the Aegean region are the most dominant sediment deliverers to the EMS. They can be considered as the dominant end-members of EMS lithic sediments and have well defined Sr–Nd isotopic signatures that allow one to trace their dominance in the sub-basins of the EMS. Sediment input from the Calabrian Arc and Adriatic Sea accounts for the substantial amount of Ionian Sea surface sediments. However, no isotope analysis of the source areas are available. To date, a limited data set for the eastern Levantine Basin outlines the Sr isotopic composition of lithogenic surface sediments (Krom et al., 1999a). In order to cover the entire EMS and to refine scenarios of dispersal pattern in this study, we present $^{143}Nd/^{144}Nd$ and $^{87}Sr/^{86}Sr$ isotope ratios of lithogenic

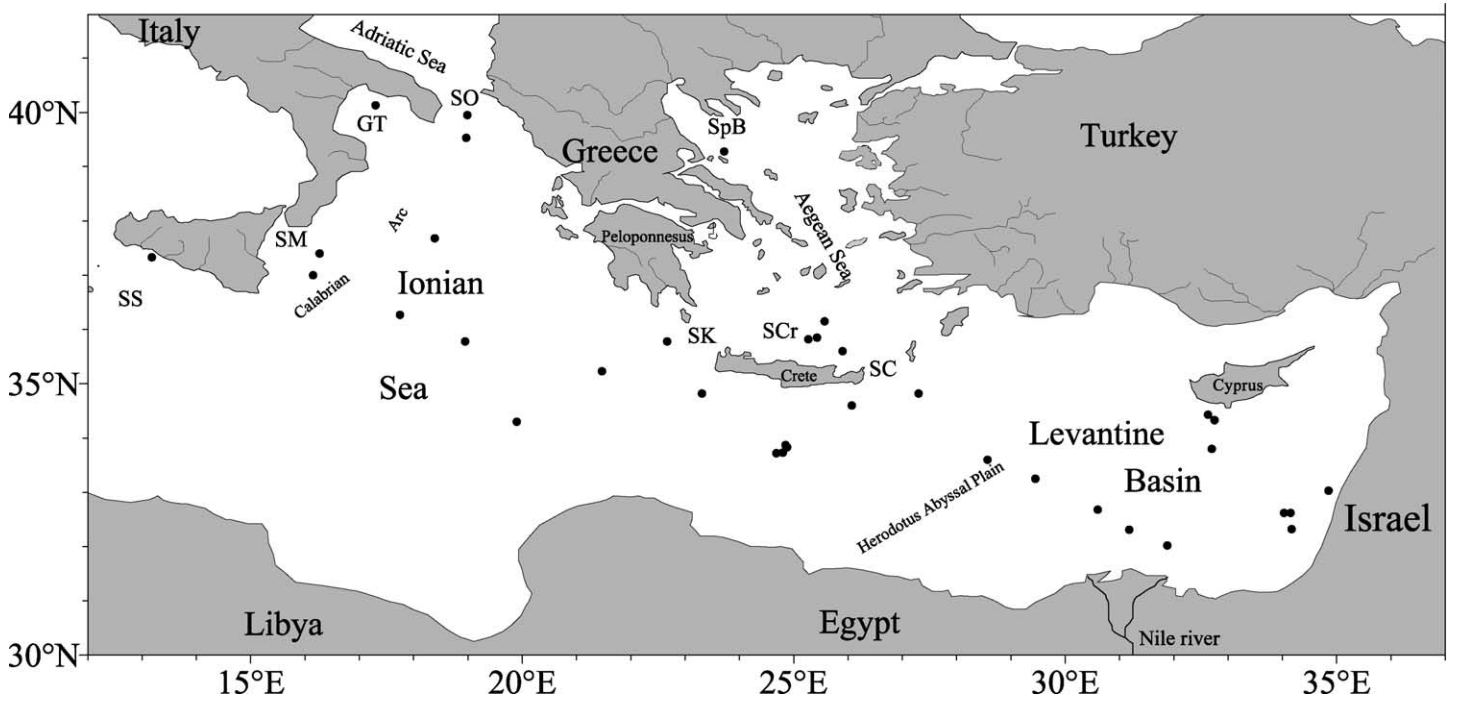

Fig. 1. Sample locations (dots) and name of localities mentioned in the text: SS = Strait of Sicily, SM = Strait of Messina, GT = Gulf of Taranto, SO = Strait of Otranto, SK = Strait of Kithira, SpB = Sporades Basin, SCr = Sea of Crete, SC = Strait of Casos.

surface sediments covering all important entrances and basins of the EMS (Fig. 1). The analysis of the $^{143}Nd/^{144}Nd$ isotope is less influenced by grain size variation that have been reported for Sr isotopes (among others Dasch, 1969; Biscaye et al., 1997). Thus, the results of the combined analyses precisely characterize the lithogenic surface sediments, constrain sediment provenance, and trace possible pathways of riverine suspended matter. Furthermore, our results are useful for the isotope-based interpretation of climate induced variations of lithogenic sediments in the EMS.

Table 1
Sr- and Nd-isotopic composition of bulk lithogenic surface sediments from the EMS

Sample	Location	Latitude N	Longitude E	Water depth (m)	$^{87}Sr/^{86}Sr$ ($\pm 2\sigma \times 10^{-6}$)	$^{143}Nd/^{144}Nd$ ($\pm 2\sigma \times 10^{-6}$)	$\varepsilon_{Nd(0)}$
KL60	S. of Sicily	37°20.15	13°11.33	470	0.715700 (10)	0.512017 (07)	− 12.11
MC536	G. of Messina	37°23.65	16°00.37	2850	0.720086 (10)	0.512079 (10)	− 10.90
MC533	G. of Messina	37°00.21	16°09.38	2718	0.717931 (10)	0.512065 (09)	− 11.18
MC10	G. of Taranto	40°08.29	17°01.84	1100	0.716945 (10)	0.512123 (07)	− 10.01
964A	Ionian Sea	36°15.62	17°44.99	3657	0.717057 (10)	0.512015 (08)	− 12.15
973A	Ionian Sea	35°46.82	18°56.88	3695	0.716977 (10)	0.512018 (08)	− 12.09
MC531	S. of Otranto	39°31.70	18°58.27	832	0.716887 (10)	0.512143 (09)	− 9.66
MC532	S. of Otranto	39°56.78	18°59.95	910	0.717533 (10)	0.512145 (10)	− 9.62
KL55	Ionian Sea	34°18.15	19°53.92	3129	0.717430 (10)	0.511995 (08)	− 12.54
MC534	Ionian Sea	35°13.83	21°28.29	3515	0.715924 (10)	0.512076 (09)	− 10.96
KL59	Ionian Sea	35°48.63	22°40.22	1012	0.716473 (10)	0.512074 (08)	− 11.00
SL71	SW of Crete	34°48.61	23°11.66	2827	0.71695 (10)	0.512051 (10)	− 11.45
MC515	Sporades B.	39°16.49	23°42.97	1250	0.713245 (10)	0.512247 (08)	− 7.63
971A	S of Crete	33°43.62	24°40.83	2037	0.715968 (10)	0.51207 (10)	− 11.08
970A	S of Crete	33°44.19	24°48.12	2087	0.716211 (10)	0.512077 (10)	− 10.94
KL53	S of Crete	33°51.58	24°51.46	2165	0.716395 (10)	0.512067 (10)	− 11.14
969A	S of Crete	33°50.46	24°52.98	2200	0.716119 (10)	0.512062 (07)	− 11.24
MC521	Sea of Crete	35°49.01	25°15.97	1839	0.713724 (10)	0.512217 (09)	− 8.21
MC522	Sea of Crete	35°50.52	25°25.99	1840	0.713734 (10)	0.512206 (07)	− 8.43
KL49	Sea of Crete	36°08.76	25°33.84	828	0.713831 (10)	0.512209 (10)	− 8.37
KL50	Sea of Crete	35°35.99	25°54.33	560	0.710914 (10)	0.512341 (09)	− 5.79
SL67	SE of Crete	34°48.83	27°17.77	2157	0.714959 (10)	0.512152 (09)	− 9.48
MC21	Levantine B.	33°36.29	28°34.26	3039	0.714361 (10)	0.512157 (08)	− 9.34
MC22	Levantine B.	33°14.70	29°27.27	2948	0.714213 (10)	0.51215 (10)	− 9.48
MC23	Levantine B.	32°40.79	30°35.81	1940	0.710944 (10)	0.512367 (10)	− 5.25
MC24	Levantine B.	32°19.45	31°10.49	1007	0.709495 (10)	0.512468 (09)	− 3.28
MC25	Levantine B.	32°00.54	31°53.25	199	0.708426 (10)	0.512441 (08)	− 3.80
MC38	Levantine B.	34°26.06	32°37.60	2473	0.712306 (10)	0.51244 (10)	− 3.82
966A	Levantine B.	33°47.79	32°42.09	926	0.711386 (10)	0.512289 (08)	− 6.81
968A	Levantine B.	34°19.90	32°45.06	1961	0.710862 (10)	0.512312 (11)	− 6.36
KL85	Levantine B.	32°36.81	34°01.62	1450	0.709381 (10)	0.512485 (10)	− 2.98
KL83	Levantine B.	32°36.87	34°08.89	1431	0.711353 (10)	0.512472 (08)	− 3.24
KL82	Levantine B.	32°19.31	34°09.93	1284	0.709053 (10)	0.512495 (08)	− 2.79
MC35	Levantine B.	33°01.55	34°50.62	1028	0.707531 (10)	0.512583 (10)	− 1.03
Average value of Aegean Tertiary basalts[a]					0.707610	0.512476	− 3.12
Average value of Nile river sediments[b]					0.707043	0.512469	− 3.25
Average value of Saharan dust[c]					0.721788	0.511969	− 13.00

B. = Basin, G. = Gulf, S. = Strait, S = South, SE = Southeast, SW = Southwest.

[a] Data from Güleç (1991).

[b] Data from Goldstein et al. (1984) and Krom et al. (1999a).

[c] Data from Grousset et al. (1998).

2. Sampling and analytical procedures

Surface sediments were recovered during four cruises of the German research vessel ''Meteor'' (M25/3 in 1993, M40/3 and M40/4 in 1998, M44/3 in 1999) and the ODP Leg 160 (Emeis et al., 1996). The uppermost centimeter of the cores was subsampled. The samples were oven-dried at 105 °C for 48 h; subsequently, the samples were grounded and homogenized.

The surface sediments from the vicinity of Sicily/southwest Italy and Nile delta are dominated by aluminosilicates and contain between 17 and 22 wt.% carbonates (data not shown in this work). The samples around Crete and from the centres of the sub-basins have carbonate contents between 48 and 57 wt.%. Because of the oligotrophic condition of the EMS and utilisation/dissolution, the contents of organic matter and biogenic silica in the surface sediments are negligibly low (Bethoux, 1989; Kemp et al., 1999; Struck et al., 2001). The fraction of authigenic clay mineral, Mn-/Fe-oxides, can be considered low because of high terrigenous input.

Given that the contents of organic matter and biogenic silica are very low, lithogenic sediments are defined in this work as the residues after leaching the carbonate fraction.

For radiogenic isotope analysis of the bulk lithogenic fractions, 500 mg of powdered and homogenized sediment were leached with 10 ml acetic acid (5 M) at room temperature for 12 h. The detrital residue was rinsed several times with deionized water and centrifuged. Afterwards, the water was pipetted off. Fifty milligrams of the dried residue was spiked with a mixed $^{149}Sm/^{150}Nd$ spike prior to digestion in HF. The digested samples were dried and dissolved in 6 N HCl, dried and then redissolved in 2.5 HCl. For isotope analyses, Sr and light rare-earth elements were isolated on quartz columns by conventional ion exchange chromatography with a 5-ml resin bed of Bio Rad AG 50W-X12, 200–400 mesh. Nd was separated from other rare-earth elements on quartz columns using 1.7-ml Teflon powder coated with HDEHP, di(2-ethylhexyl)orthophosphoric acid, as cation exchange medium. The $^{87}Sr/^{86}Sr$ and $^{143}Nd/^{144}Nd$ ratios were determined on a Finnigan MAT 262 mass spectrometer using static collection mode at the Institute for Mineralogy, Petrology and Geochemistry, University of Tübingen. The analysis of standard NBS-SRM 987 for Sr yielded $^{87}Sr/^{86}Sr = 0.710236 \pm 08$ (2σ, $n = 41$) and standard Ames-Metal for Nd yielded $^{143}Nd/^{144}Nd = 0.512124 \pm 07$ (2σ, $n = 41$). The result of blank measurements are 100–150 pg for Nd and 100–120 pg for Sr. $^{87}Sr/^{86}Sr$ ratios are relative to $^{86}Sr/^{88}Sr = 0.1194$ and $^{143}Nd/^{144}Nd$ ratios to $^{146}Nd/^{144}Nd = 0.7219$. $^{143}Nd/^{144}Nd$ ratios are expressed as:

$$\varepsilon_{Nd(0)} = \left[\frac{(^{143}Nd/^{144}Nd)_{measured}}{(^{143}Nd/^{144}Nd)^{0}_{CHUR}} - 1 \right] \times 10^4$$

using the present-day ''chondritic uniform reservoir''(CHUR) value (0.512636) of Jacobson and Wasserburg (1980).

3. Results

The results of Nd- and Sr-isotopic analysis are shown in Table 1 and Figs. 2, 3 and 4a,b. The isotopic composition of the lithogenic sediments in the EMS reveals three provenance areas and a general E–W gradient (Fig. 2). The ratios of $^{87}Sr/^{86}Sr$ are lowest and the values of $\varepsilon_{Nd(0)}$ highest in the area northeast of the Nile cone and off Israel. From there, the $^{87}Sr/^{86}Sr$ ratios gradually increase and the $\varepsilon_{Nd(0)}$ values decrease towards the Mediterranean Ridge. The eastern flank of the Mediterranean Ridge is characterized by higher Sr isotope ratios and lower $\varepsilon_{Nd(0)}$ values. West of the eastern flank of the Mediterranean Ridge, $^{87}Sr/^{86}Sr$ ratios are lower due to material entering from the Aegean. $^{87}Sr/^{86}Sr$ ratios from the Sea of Crete and Sporades Basin (Figs. 2 and 3) show ratios comparable to those of the western Levantine Basin. The influx of material from the Aegean Sea is suggested by the isotope ratios of samples from the southeast and southwest of Crete, which display, though attenuated, ''Aegean Sea'' signatures. Samples from the Strait of Otranto are marked by moderate $^{87}Sr/^{87}Sr$ ratios and $\varepsilon_{Nd(0)}$ values, while samples from the Strait of Messina and Gulf of Taranto display the highest $^{87}Sr/^{87}Sr$. The isotopic pattern of the Ionian Sea incorporates signatures from the outflow of the Adriatic Sea, Aegean Sea, Gulf of Taranto, Strait of

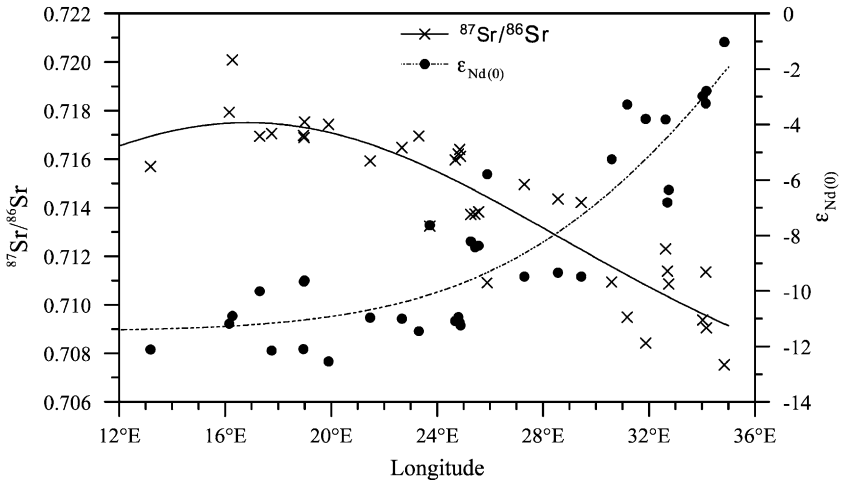

Fig. 2. Variations of $^{87}Sr/^{86}Sr$ ratios and $^{143}Nd/^{144}Nd$ ratios, expressed as $\varepsilon_{Nd(0)}$ values, in the lithogenic surface sediments of the Eastern Mediterranean Sea versus longitude. Error bars are smaller than symbols. Curve of nonlinear fit is shown.

Messina, and the Strait of Sicily. Turbid flow from both the African margin and Calabrian Rise may also contribute a significant amount of sediment. The Nd-isotopic composition of most samples is generally opposite to the Sr-isotope, displaying highest values in the easternmost part of the Levantine Basin and lowest values in the Ionian Sea (Figs. 2 and 3). The isotopic ratios of the Strait of Messina samples deviate

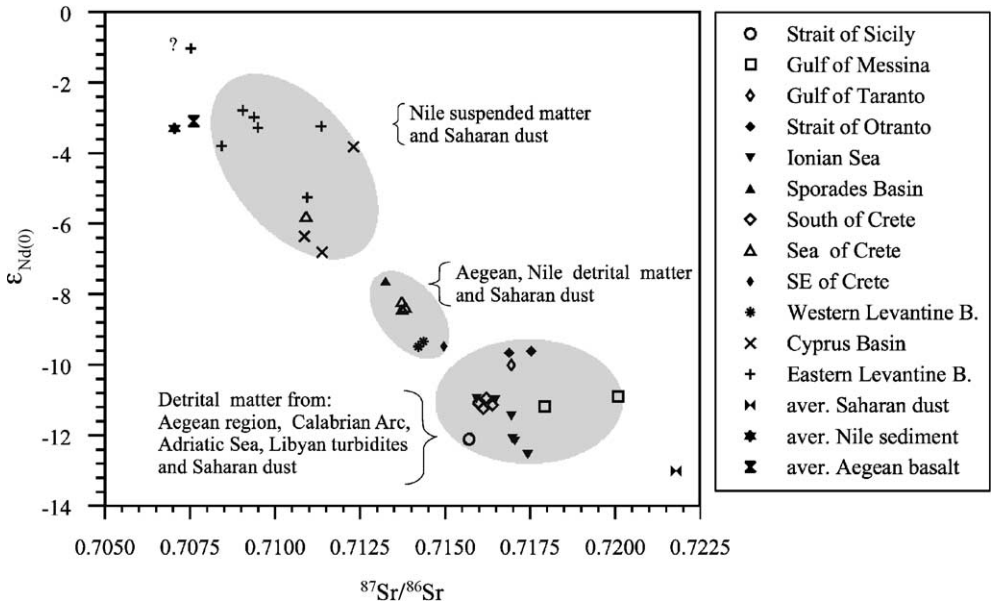

Fig. 3. $^{87}Sr/^{86}Sr$ ratios versus $^{143}Nd/^{144}Nd$ ratios, expressed as $\varepsilon_{Nd(0)}$ values, of the lithogenic surface sediments from the Eastern Mediterranean Sea. $\varepsilon_{Nd(0)}$ values and $^{87}Sr/^{86}Sr$ ratios of average Saharan dust from Grousset et al. (1998), average of Tertiary Aegean basalt from Güleç (1991), average Nile sediments from Goldstein et al. (1984) for $\varepsilon_{Nd(0)}$, and Krom et al. (1999a) for $^{87}Sr/^{86}Sr$ data. Shaded areas and accompanying text indicate provenance and main sources of terrigenous sediments.

from the pattern described above, as they show the highest $^{87}Sr/^{86}Sr$ ratios but not the lowest $\varepsilon_{Nd(0)}$ values (Fig. 2).

4. Discussion and interpretation

The isotope variability of the lithogenic surface sediments is attributed to the geochemical characteristic and the amount of material entering the EMS via rivers and distribution by currents. This is because the Saharan dust flux, though high, is in an E–W direction more or less uniform within the EMS (Rutten et al., 2000) and is isotopically more or less homogenous (Krom et al., 1999a). The average $^{87}Sr/^{86}Sr$ ratio and average $\varepsilon_{Nd(0)}$ value of Saharan dust are 0.72179 and −13.01, respectively (Grousset et al., 1998). The isotopic pattern of the eastern Mediterranean lithogenic surface sediments shows a pronounced E–W gradient (Figs. 2 and 3). The easternmost part of the Eastern Mediterranean Sea is characterized by the highest $\varepsilon_{Nd(0)}$ values and lowest $^{87}Sr/^{86}Sr$ ratios, whereas the western part of the basin displays the highest $^{87}Sr/^{86}Sr$ ratios and lowest ε_{Nd} values. Krom et al. (1999a) presented $^{87}Sr/^{86}Sr$ ratios of lithogenic sediments from the Levantine Basin and semiquanti-

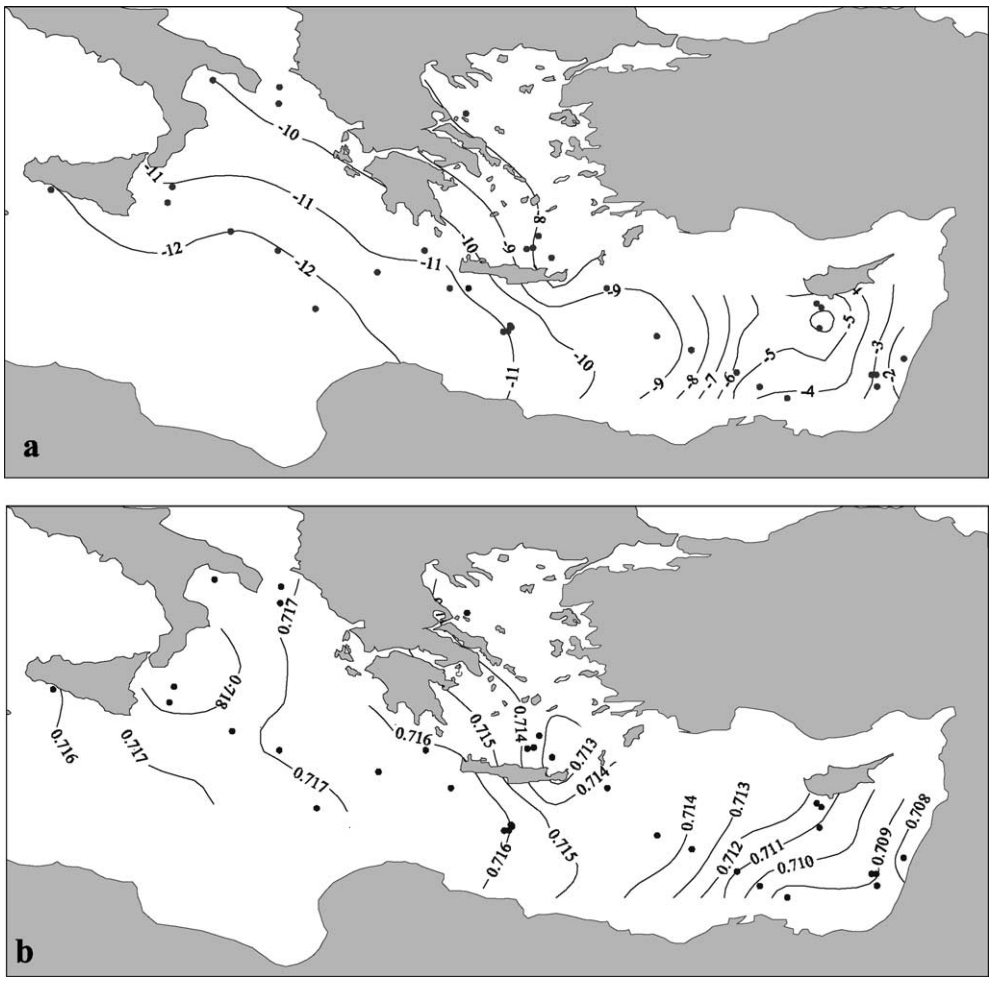

Fig. 4. Contour diagrams for the isotopic composition of lithogenic surface sediments. (a) $^{143}Nd/^{144}Nd$ ratios expressed as $\varepsilon_{Nd(0)}$ values and (b) $^{87}Sr/^{86}Sr$ ratios. Contours are drawn at intervals of 0.001.

tatively outlined the dilution of Nile sediment towards the western Levantine Basin. Our results indicate a similar distribution pattern of $^{87}Sr/^{86}Sr$ ratios in this area. However, in some sample locations that are identical to those of Krom et al. (1999a), our $^{87}Sr/^{86}Sr$ ratios are slightly lower. We attribute these variations to the different leaching procedures applied. Their treatment procedure involved ashing the samples at 450 °C before leaching using 1.25 N hydrochloric acid. Based on the distribution pattern of Sr–Nd isotopes, three provenance can be recognized (Fig. 3), namely the Levantine Basin, areas enveloping the island of Crete, and the Ionian Sea.

Samples from offshore Israel, where sedimentation is mainly influenced by the Nile sediment loads, show the most radiogenic $\varepsilon_{Nd(0)}$ values and the lowest $^{87}Sr/^{86}Sr$ ratios measured in the EMS. From this isotopic composition, it is evident that the relative contribution of Saharan dust (characterized by high $^{87}Sr/^{86}Sr$ and low $\varepsilon_{Nd(0)}$ values; Grousset et al., 1998) in this part of the sub-basin is very low. Taking into account that the Saharan dust flux in southern coastal areas of the EMS can be considered as high, the observed pattern is a reflection of the predominant role of the river Nile in this part of the Levantine Basin. This is particularly evident for the samples from the eastern Levantine Basin (Fig. 3), which plot close to the data from average Nile sediments (Goldstein et al., 1984; Krom et al., 1999a). This distribution pattern of isotopic signature reflects the surface water current in the easternmost Levantine Basin (Pinardi and Masetti, 2000). The Nile suspended matter is first deflected along the Egyptian–Israel coast. South and north of Cyprus, the dispersal turns westward, as shown in this paper and in previous work (Venkatarathnam and Ryan, 1971). Furthermore, the data reveal that the contribution of Nile sediment decreases significantly towards the west (Figs. 2, 3 and 4a,b). Turbid flows from the North African shelf may have been partially responsible for the dilution of the Nile suspended matter. Turbid flows from the Libyan–Egyptian margin contribute a significant amount of sediment to the Herodotus Abyssal Plain (Cita et al., 1984; Reeder et al., 1998). The surface sediments of the eastern flank of the Mediterranean Ridge, a morphological high, are not influenced by the Nile sediment load and display values close to those of eolian sediments (Krom et al., 1999a). Samples from the Sporades Basin and Sea of Crete, both in the Aegean Sea, have isotopic compositions that are similar to those of the central Levantine Basin. Their source are Aegean volcanic rocks, which are marked by high $\varepsilon_{Nd(0)}$ values and low $^{87}Sr/^{86}Sr$ ratios (Güleç, 1991), chernozoemic soil, and andesitic rocks exposed in the watershed areas (McCoy, 1974). While their isotopic signatures envelop the island of Crete,

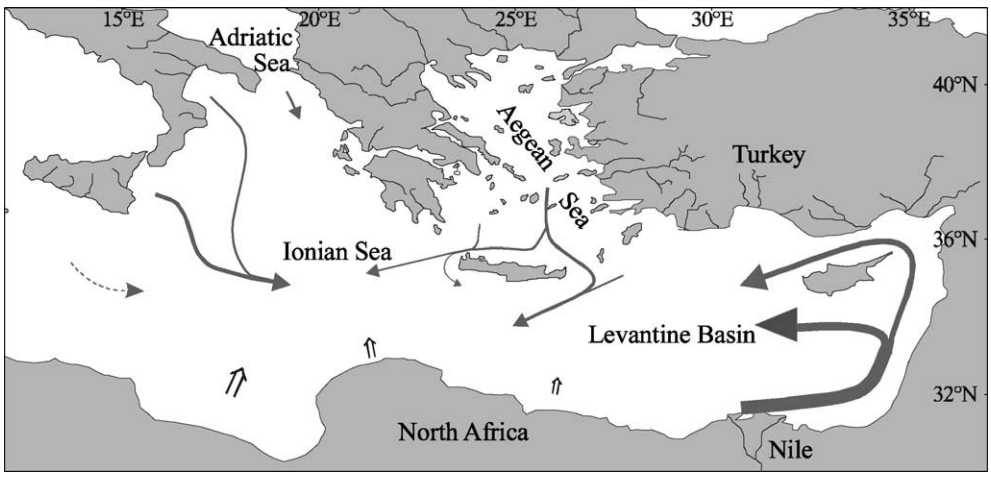

Fig. 5. Schematic depiction of main pathways of riverine suspended matters. Turbid flows from the North African margin (open arrows) are indicated after Reeder et al. (1998).

the pattern suggests that the dispersion of lithogenic components from the Aegean Sea entering into the EMS is mainly through the Strait of Casos to the east of Crete (Figs. 4a,b and 5), reflecting the role of the intermediate water from the Aegean Sea (Schlitzer et al., 1991). The "Aegean" signal is diluted faster in the Strait of Kithira to the west of Crete and southwestwards into the Ionian Sea. This is probably related with the amount and strength of the water masses and currents entering into the EMS via this strait, respectively. Alternatively, the Aegean signal, in the area northwest of Crete, may be masked by the erosion products from the Peloponnesus Peninsula. However, the sediment contribution of the Peloponnesus Peninsula may be assumed to be minimal because the watershed is small and significant rivers are absent in this area (Fig. 1). In our interpretation, the dilution gradient reflects the relative importance of the two straits for near-floor sediment transport.

The lithogenic supply to the Ionian Sea is derived from several sources. Material of Aegean origin is diluted quickly by outflow from the Adriatic Sea, which is supplied mainly by the river Po and other rivers draining adjacent areas. The Calabrian Arc on the southern Italian Peninsula is a localised source with specific Sr- and Nd-isotope signatures. Samples from the Ionian Sea show $^{87}Sr/^{86}Sr$ ratios that are closer to those of the Strait of Otranto and Strait of Messina (Fig. 4a). In the northern and northwestern Ionian, the sediment distribution is dominated by deep water currents that spread out southward from the Adriatic Sea via the Strait of Otranto (Schlitzer et al., 1991). However, our sample set lacks samples from the Libyan shelf, which is also a dominant supplier of terrigenous sediment to the Eastern Mediterranean Sea (Cita et al., 1984; Reeder et al., 1998). Turbidite sediments from the Libyan shelf display $\varepsilon_{Nd(0)}$ values (Freydier et al., 2001) very similar to the values of the Ionian Sea surface sediments (Fig. 2).

5. Conclusions

Based on the Sr- and Nd-isotope composition of the lithogenic components of the surface sediments and the geology of the catchment areas, we provide a characterization of the lithogenic surface sediments and delineate provenances as well as possible pathways of the riverine/current suspended matter (Fig. 5). The patterns displayed in Fig. 5 fairly reflect the surface currents in the eastern most Levantine Basin, the surface and intermediate currents entering into EMS from the Aegean Sea, and the deep water current into the Ionian Sea from the Adriatic Sea entering. The Nile sediment load is deflected along the Egyptian–Israel coast and subsequently directed towards the west. The compositional influence of the Nile sediment load decreases rapidly from the Nile cone towards the west and is barely traceable at the eastern flank of the Mediterranean Ridge. In the Herodotus Abyssal Plain, the Nile signature may be diluted by occasional turbid flows from the Libyan–Egyptian margin. The eastern flank of the Mediterranean Ridge itself is characterized by isotopic values that are very similar to those of the Saharan dust collected above the eastern Mediterranean (Krom et al., 1999a). This implies that it does not receive significant amount of Nile sediments. Sediment load entering the EMS via the Aegean Sea is generally low and it spreads out mainly through the Strait of Casos. Passing through the strait, the detrital dispersions are deflected towards the south of the island of Crete (Fig. 5). The amount of sediment entering the EMS via the Strait of Kithira appears to be much lower compared to those entering through the Strait of Casos. Thus, its isotopic trace is obliterated faster towards the Ionian Sea. Furthermore, a southeastward deflection is evident, but its southeastward spread seems very limited (Figs. 4a,b and 5). Sediment suspensions from the Adriatic Sea and the region of the Messina cone first spread out in a southern direction and then are channelled towards the central Ionian Sea. Turbidities from the African margin also represent important sediment suppliers to the Ionian Sea.

Acknowledgements

We thank the crew of the R/V Meteor for their help and assistance, ODP for making sample material available, Dr. H. Schulz (Institute for Baltic Sea Research) for support during subsampling, Dr. R. Wehausen for critical reading of an earlier version of this manuscript, Dr. J. Pross for improving the English, and E. Reitter for the isotope analyses. We are also grateful to the reviewers, Dr. M. Krom and

Dr. M. Revel, for thoughtful revisions of the manuscript and constructive comments. This work was funded by the Deutsche Forschungsgemeinschaft grants to Emeis (Em 37/8) and Hemleben (697/28).

References

Aksu, A.E., Yasar, D., Mudie, P.J., 1995. Origin of the late glacial–Holocene hemipelagic sediments in the Aegean Sea: clay mineralogy and carbonate cementation. Mar. Geol. 123, 33–59.

Bethoux, J.-P., 1989. Oxygen consumption, new production, vertical advection and environmental evolution in the Mediterranean Sea. Deep-Sea Res. 36, 769–781.

Biscaye, P.E., Grousset, F.E., Revel, M., Van der Gaast, S., Zielinski, G.A., Vaars, A., Kukla, G., 1997. Asian provenance of glacial dust (stage 2) in the Greenland Ice Sheet Project 2 Ice Core, Summit, Greenland. J. Geophys. Res. 102, 26765–26781.

Chester, R., Baxter, G.G., Behairy, A.K.A., Nonnor, K., Cross, D., Elderfield, H., Padgham, R.C., 1977. Soil-sized eolian dusts from the lower troposphere of the Eastern Mediterranean Sea. Mar. Geol. 24, 201–217.

Cita, M.B., Camerlenghi, A., Kastens, K.A., McCoy, F.W., 1984. New findings of Bronze Age homogenites in the Ionian Sea: geodynamic implications for the Mediterranean. Mar. Geol. 55, 47–62.

Cramp, A., O'Sullivan, G., 1999. Neogene sapropels in the Mediterranean: a review. Mar. Geol. 153, 11–28.

D'Almeida, G.A., 1986. A model for Saharan dust transport. J. Clim. Appl. Meteorol. 25, 903–916.

Dasch, E.J., 1969. Strontium isotopes in weathering profiles, deep-sea sediments, and sedimentary rocks. Geochim. Cosmochim. Acta 33, 1521–1552.

Emeis, K.-C., Robertson, A.H.F., Richter, C., et al., 1996. Proceeding of the ODP, Initial Reports. 160, College Station, TX (Ocean Drilling Program).

Emeis, K.-C., Sakamoto, T., Wehausen, R., 2000. The sapropel record of the eastern Mediterranean Sea—results of Ocean Drilling Program Leg 160. Palaeogeogr., Palaeoclimatol., Palaeoecol. 158, 371–395.

Foucault, V.A., Stanley, D.J., 1989. Late Quaternary palaeoclimatic oscillation in East Africa recorded by heavy minerals in the Nile delta. Nature 339, 44–46.

Freydier, R., Michard, A., De Lange, G., Thomson, J., 2001. Nd isotopic compositions of Eastern Mediterranean sediments: tracers of the Nile influence during sapropel formation? Mar. Geol. 177, 45–62.

Goldstein, S.L., O'Nions, R.K., Hamilton, P.J., 1984. A Sm-Nd isotopic study of atmospheric dusts and particulates from major river systems. Earth and Planetary Science Letters 70, 221–236.

Grousset, F.E., Parra, M., Bory, A., Martinez, P., Bertrand, P., Shiemmield, G., Ellam, R.M., 1998. Saharan wind regimes traced by the Sr–Nd isotopic composition of subtropical Atlantic sediments: Last Glacial maximum vs. today. Quat. Sci. Rev. 17, 395–409.

Guerzoni, S., Molinaroli, E., Chester, R., 1997. Saharan dust input to the western Mediterranean Sea: depositional patterns, geochemistry and sedimentology implications. Deep-Sea Res. 44, 631–654.

Güleç, N., 1991. Crust–mantle interaction in western Turkey: implications from Sr and Nd isotope geochemistry of tertiary and quaternary volcanics. Geol. Mag. 128, 417–435.

Jacobson, S.B., Wasserburg, G.J., 1980. Sm–Nd isotopic evolution of chondrites. Earth Planet. Sci. Lett. 50, 139–155.

Kemp, A.E.S., Pearce, R.B., Koizumi, I., Pike, J., Rance, S.J., 1999. The role of mat-forming diatoms in the formation of Mediterranean sapropels. Nature 398, 57–61.

Krom, M.D., Cliff, R.A., Eijsink, L.M., Herut, B., Chester, R., 1999a. The characterisation of Saharan dusts and Nile particulate matter in surface sediments from the Levantine basin using Sr isotopes. Mar. Geol. 155, 319–330.

Krom, M.D., Michard, A., Cliff, R.A., Strohe, K., 1999b. Source of sediment in the Ionian Sea and western Levantine basin of the Eastern Mediterranean during S-1 sapropel times. Mar. Geol. 160, 45–61.

McCoy, F.W., 1974. Late Quaternary sedimention in the Mediterranean Sea. PhD Thesis, Harvard University, Cambridge, 132 pp.

Pinardi, N., Masetti, E., 2000. Variability of the large general circulation of the Mediterranean Sea from observations and modelling: a review. Palaeogeogr., Palaeoclimatol., Palaeoecol. 158, 153–173.

Reeder, M., Rothwell, R.G., Stow, D.A.V., Kahler, G., Kenyon, N.H., 1998. Turbidite flux, architecture and chemostratigraphy of the Herodotus Basin, Levantine Basin, SE Mediterranean Sea. In: Stoker, M.S., Evans, D., Cramp, A. (Eds.), Geological Processes on Continental Margin: Sedimentation, Mass-Wasting and Stability. Geological Society Special Publication, vol. 129, pp. 19–42.

Rutten, A., de Lange, G.D., Ziveri, P., Thomson, J., van Santvoort, P.J.M., Colley, S., 2000. Recent terrestrial and carbonate fluxes in the pelagic eastern Mediterranean; a comparison between sediment trap and surface sediment. Palaeogeogr., Palaeoclimatol., Palaeoecol. 158, 197–213.

Schlitzer, R., et al., 1991. Chlorofluoromethane and oxygen in the Eastern Mediterranean Sea. Deep-Sea Res. 38, 1531–1551.

Stanley, D.J., Wingerath, J.G., 1996. Clay mineral distributions to interpret Nile cell provenance and dispersal: I. Lower river to delta sector. J. Coast. Res. 12, 911–929.

Stanley, D.J., Mart, Y., Nir, Y., 1997. Clay mineral distributions to interpret Nile cell provenance and dispersal: II. Coastal plain from Nile delta to northern Israel. J. Coast. Res. 13, 506–533.

Stanley, D.J., Nir, Y., Galili, E., 1998. Clay mineral distributions to interpret Nile cell provenance and dispersal: III. Offshore margin between Nile and Northern Israel. J. Coast. Res. 14, 196–217.

Struck, U., Emeis, K.-C., Voß, M., Krom, M.D., Rau, G.H., 2001. Biological productivity during sapropel formation in the eastern Mediterranean Sea: evidence from stable isotopes of nitrogen and carbon. Geochim. Cosmochim. Acta. 65, 3249–3266.

Tomadin, L., Lenanz, R., Landuzzi, V., Mazzucotelli, A.,Vannucci,

R., 1984. Wind-blown dusts over the Central Mediterranean. Oceanol. Acta 7, 13–23.

Venkatarathnam, K., Ryan, W.B.F., 1971. Dispersal patterns of clay minerals in the sediments of the Eastern Mediterranean Sea. Mar. Geol. 11, 261–282.

Weldeab, S., Emeis, K.-C., Hemleben, C., Vennemann, W.T., in press. Sr-, Nd-isotopic and geochemical composition of Late Pleistocene sapropels and non-sapropel sediments from the Eastern Mediterranean Sea: implications for detrital flux and climatic conditions in the source areas. Geochim. Cosmochim. Acta.